AAS 679

CHARACTERIZING THE INFLUENCE OF STOCHASTIC FORCES ON THE DYNAMICS AROUND NON-SPHERICAL BODIES.

Iosto Fodde[*], Lucia Francesca Civati[*], and Fabio Ferrari[*]

Within astrodynamics and celestial mechanics there are various systems which cannot be modelled by just a purely deterministic system but have to include stochastic processes. These can be, for example, movements of spacecrafts through small space debris clouds or the dynamics of moonlets within rings. This work investigates how the dynamics in complex environments including various types of perturbations and stochastic processes can be characterised. For this, a dynamical polynomial chaos expansion is used, together with a novel type of stochastic chaos indicator called the pseudo-diffusion exponent. The resonant dynamics around asteroid Didymos is investigated using this tool, specifically looking at how the dynamics around the 3:1 resonance changes for different stochasticity levels. The results show that for larger levels of stochasticity, representing for example higher velocity relative impacts and a larger number of impacts, can result in reduced stability within these resonances. In general, the results presented here show how stochastic processes in celestial mechanics and astrodynamics can be efficiently characterised.

INTRODUCTION

Most systems in astrodynamics and celestial mechanics are modeled from a deterministic point of view, where the dynamics can be described by a system of ordinary differential equations (ODE), like for the two- or three-body problem. When uncertainty is introduced, most often this is implemented through parametric uncertainty in the initial state and/or the system variables. However, there are several important systems within the field of astrodynamics and celestial mechanics that cannot be modeled through only a deterministic ODE.

An example of this type of system is a spacecraft moving through a cloud of particles that have a random distribution of velocities. This results in the spacecraft experiencing (non-destructive) impacts with these particles that then impart a random $\Delta\mathbf{v}$ on the spacecraft. This happens for satellites around Earth when moving through a cloud of debris fragments,[1] or for a cloud of debris itself as impacts between the individual fragments cause the cloud to diffuse over time. Another potential stochastic process is the effect of ejecta from small solar-system bodies (SSBs) on a spacecraft moving around it. This can be the ejecta cloud stemming from the outgassing of a comet, but also asteroids that release ejecta through other processes have been detected recently

[*]Department of Aerospace Science and Technology (DAER), Politecnico di Milano, Via La Masa 34, Milan, Italy

(see for example the observations of OSIRIS-Rex of ejecta from Bennu, or the asteroid Phaethon, which is believed to be the parent asteroid of the Gemini meteor shower and target of the upcoming Destiny+ mission). This type of scenario is especially relevant for the upcoming Hera mission which will perform close-proximity operations around binary asteroid Didymos. The secondary of this system was impacted by the DART spacecraft, creating a large amount of ejecta that could potentially still remain within the system. The dynamics of several natural bodies within the Solar system have also been postulated to be influenced by stochastic processes. Examples include the evolution of planetary ring systems and the moons contained within,[2] the migrations of planets and moons due to impacts with planetesimals,[3] and the origin of the Moon.[4]

These examples show that there is a need for a set of tools that can help in analyzing the properties of these kind of systems. Only limited work has been done regarding this subject. In[5] the basic two-body problem was expanded to a stochastic differential equation (SDE), consisting of a deterministic central gravity part and a stochastic diffusive part, which was modeled as a Weiner process. Some basic properties could be derived for this model, such as the conditions under which energy is not conserved anymore.[6] derived Gauss' stochastic planetary equations, which allowed for the analysis of the change in the orbital elements due to the stochastic perturbation. Separately,[7] looked at how the motion in the restricted three-body problem is affected by a random walk type force. This was specifically applied to the problem of identifying the possible transition of motion around L_4 and L_5 to a horseshoe orbit and then to a possible impact with one of the primaries. All of these works used some simplifying assumptions like Gaussian probabilities and stationary processes to be able to give concrete conclusions, which limit their applicability to a wider range of problems.[8] first introduced the use of high-order expansions of the stochastic dynamics to investigate a wider range of processes. They then applied their methodology to a satellite in geostationary orbit, observing the diffusion of the system due to the stochastic force.

This work starts with a similar methodology as,[8] using expansions of the stochastic dynamics, but will extend this methodology to be able to better characterize the full phase space of the system and apply it to more complex, nonlinear, dynamical systems.

DYNAMICS

Stochastic Differential Equations

First, a general stochastic differential equation (SDE) can be formulated as follows:

$$d\mathbf{X}(t,\omega) = \mathbf{f}(\mathbf{X}(t,\omega),t)dt + \mathbf{G}(\mathbf{X}(t,\omega),t)dW(t,\omega), \tag{1}$$

where $\mathbf{X}$ is the random state vector, $\mathbf{f}(\mathbf{X},t)$ the deterministic dynamics, also known as the drift, $\mathbf{G}(\mathbf{X},t)$ represents the noise function, also known as the diffusion, and dW is the stochastic noise process. Here, ω represents the fact that $\mathbf{X}$ is a random variable and individual realisations of ω represent different trajectories of the stochastic process dW. The properties of $\mathbf{G}(\mathbf{X},t)$ and dW can be chosen based on the specific system, and can be generally non-Gaussian and non-stationary. In case the process represents a series of small accelerations with frequency much higher than the characteristic frequency of f, a Wiener process can be used according to the central limit theorem. For cases where the jumps are less frequent or perhaps dependent of each other, other types like Poisson or Levy flights can be used.

The SDE of Eq. (1) has a corresponding integral equation:

$$\mathbf{X}(t,\omega;\mathbf{X}_0) = \mathbf{X}_0 + \int_0^t \mathbf{f}(\mathbf{X}(s,\omega),s)ds + \int_0^t \mathbf{G}(\mathbf{X}(s,\omega),s)dW(s,\omega), \tag{2}$$

where the second integral is an Itô integral. Some basic properties of these types of equations and their solutions can be found in.[9] Most SDEs, especially if they are nonlinear, do not have analytical solutions. Therefore, path-wise solutions are mostly obtained through numerical schemes, e.g. a first order approximation can be made using the Euler-Maruyama scheme, an extension of the Euler scheme used for ODEs. Higher order schemes are also available,[10] but they still only provide path-wise solutions and other methods need to be used to propagate the full probability density information.

Stochastic Processes in Space Dynamics

As discussed in the introduction, this work aims to present a general framework which can characterise stochastic dynamical systems, especially systems where stochastic processes are important. Thus, it is important to highlight the wide variety of systems where the stochastic process cannot be ignored and hence where this methodology might be of use. A summary of these systems is given in Table 1.

With regards to celestial mechanics, there are several processes that have been observed to be influenced significantly by stochastic effects. In most of these cases there is an interaction of a larger body with a large amount of smaller particles, like in a planetary ring,[11] or with a more continuous medium, like a proto-planetary disk.[12] In the latter case the main stochastic effects come from interactions with density disturbances in the medium, while in the former they can be both due to collisional and gravitational interactions. Other examples of stochastic processes in celestial mechanics can be observed in minor bodies interacting with larger planets, for example changing the binary orbits of Kuiper belt objects[13] or in their capture in mean motion resonances.[14]

The dynamical evolution of space debris contains several stochastic processes. This can be observed in the evolution of a cloud of debris, interacting with itself through collisions[1] or in the drag force that evolves stochastically through both the tumbling motion of the particle and the random density fluctuations in the upper atmosphere.[15] The dynamics of a spacecraft itself has diffusive properties in certain situations as well. For example, a low-thrust spacecraft might experience a continuous stochastic component in the magnitude and direction of its thrust on top of the commanded thrust,[16] or discontinuous in case of de-saturation maneuvers.[17] Finally, some measurements of GPS satellites also suggest that Solar radiation pressure is best modelled as a stochastic process due to its complex iteraction with the different surfaces of a spacecraft.[18]

Table 1: Examples of systems where stochastic processes can play a significant role.

Physical System	**Origin of Random Process**	**Observed Effect**	**References**
Planetary and Asteroid rings.	Collisions between ring particles and their gravitational influence.	Stochastic migration of moonlets and Saturn's propellers.	11, 19, 20
Planets in Protoplanetary Disk	Disk instabilities due to magnetorotational turbulence creating gravitational torques.	Stochastic change in the orbital parameters of young planets.	3, 12, 21
Kuiper Belt Objects binary orbits.	Impulsive and isotropic encounters with other objects in the Kuiper belt.	Eccentricity and inclination of binary orbit changes according to a Lévy flight.	13
Dynamics and distribution of Kuiper Belt Objects.	Stochastic migration of Neptune and other outer planets excite objects in a random manner.	Diffusion of objects away from certain mean motion resonances.	14, 22, 23
Orbital evolution of space debris.	Impacts with other debris and micrometeorites and density fluctuations in upper atmosphere.	Diffusion of objects and changing re-entry times.	1, 15, 24
Spacecraft dynamics and maneuvering.	Stochastic error in (low-thrust) maneuvers, translational component of de-saturation maneuvers, Solar radiation pressure, etc.	Increasing dispersion in spacecraft state.	17, 18, 25

STOCHASTIC DYNAMICS INDICATOR

Polynomial Chaos

Consider a dynamical system with a set of random variables, which are collected into a vector $\boldsymbol{\xi} \in \Omega_{\boldsymbol{\xi}}$, where $\Omega_{\boldsymbol{\xi}}$ represents the, bounded or unbounded, set of uncertainty realisations. This vector can contain various types of uncertainties, e.g. initial state uncertainties, environment parametric uncertainties, etc. Later in this section, a method to convert a random process into a set of random variables that can be collected into $\boldsymbol{\xi}$ will be presented. The main concept behind polynomial chaos expansion (PCE) is that we can expand the solution of an SDE, given in Eq. (2), using an expansion of orthogonal polynomials as follows:

$$\tilde{\mathbf{X}}(t, \boldsymbol{\xi}) = P_{n,d}(\boldsymbol{\xi}) = \sum_{\mathbf{i}, |\mathbf{i}| \leq n} c_{\mathbf{i}}(t) \Psi_{\mathbf{i}}(\boldsymbol{\xi}), \tag{3}$$

where d is the degree of the polynomial, n is the number of variables of the polynomial, $\mathbf{i} \in [0, d]^n \subset \mathbb{N}^n$ is a vector of indices with $\mid \mathbf{i} \mid = i = \sum_{r=1}^{n} i_r$, $\{c_{\mathbf{i}}\}$ are a set of coefficients, and $\{\Psi_{\mathbf{i}}(\boldsymbol{\xi}) = \alpha_{i_0}(\xi_0) \cdot \alpha_{i_1}(\xi_1) \cdot ... \cdot \alpha_{i_d}(\xi_d)\}$ are multivariate basis functions generated using a tensor product of univariate polynomials. The polynomial basis functions $\{\Psi_i\}$ are orthogonal under the weight function ρ:

$$\langle \Psi_n, \Psi_m \rangle = \int \Psi_n(\boldsymbol{\xi}) \Psi_m(\boldsymbol{\xi}) \rho(\boldsymbol{\xi}) d\boldsymbol{\xi} = \langle \Psi_n^2 \rangle \delta_{n,m}. \tag{4}$$

The size of the expansion, i.e. the number of terms of the polynomial, is given by $\mathcal{N} = \binom{n+d}{d}$, where d is the maximum degree of the polynomial.

The original version of this method was called homogeneous chaos, or also Wiener chaos after the author.[26] There, Hermite polynomials were used as basis functions and a Gaussian distribution was considered. It was found that the expansion exponentially converges to the true output distribution, mainly due to the fact that the weight function ρ associated with Hermite polynomials has the same functional form as a Gaussian distribution. This idea was expanded upon in[27] to other orthogonal polynomial families which have other weight functions that are also associated to different classes of probability density functions through the so-called Askey scheme. This way, non-Gaussian distributed functions are approximated with exponential convergence as well by selecting the corresponding polynomial basis from the Askey scheme.

The coefficients $\{c_i\}$ can be found in various different ways, both using intrusive and non-intrusive methods. Here, a non-intrusive point collocation method is selected due to its found accuracy. For this method a set of Q input parameters, also known as nodes, are sampled and propagated forward through the model. Then, the following problem is solved:

$$\{c_{\mathbf{i}}\} = \arg\min_{c_{\mathbf{i}}} \sum_{k=0}^{Q} \left[f(\boldsymbol{\xi}_{\mathbf{k}}) - \sum_{\mathbf{i},|\mathbf{i}|\leq n} c_{\mathbf{i}} \Psi_{\mathbf{i}}(\boldsymbol{\xi}_{\mathbf{k}}) \right], \tag{5}$$

using a least squares regression technique by inverting the following system:

$$HC = Y, \tag{6}$$

where:

$$H = \begin{bmatrix} \Psi_{i_1}(\boldsymbol{\xi}_1) & \dots & \Psi_{i_s}(\boldsymbol{\xi}_1) \\ \vdots & \ddots & \vdots \\ \Psi_{i_1}(\boldsymbol{\xi}_s) & \dots & \Psi_{i_s}(\boldsymbol{\xi}_s) \end{bmatrix}, C = \begin{bmatrix} c_{i_1} \\ \vdots \\ c_{i_s} \end{bmatrix}, Y = \begin{bmatrix} \mathbf{y}_1 \\ \vdots \\ \mathbf{y}_s \end{bmatrix} \tag{7}$$

where $s = \mathcal{N}$, $\boldsymbol{\xi}_1, \dots, \boldsymbol{\xi}_s$ are the nodes, and Y the vector containing all the corresponding propagated samples $\mathbf{y}_i = \mathbf{X}(t, \boldsymbol{\xi}_i)$.

The resulting polynomial approximation of the solution distribution can be exploited to obtain analytical expressions of its statistical moments. For example, the mean can be obtained as follows:

$$\bar{\mathbf{X}}(t, \boldsymbol{\xi}) = \mathbb{E}[\mathbf{X}(t, \boldsymbol{\xi})] \approx \mathbb{E}[P_{n,d}(t, \boldsymbol{\xi})] = \int_{\Omega_{\boldsymbol{\xi}}} \left(\sum_{\mathbf{i},|\mathbf{i}|\leq n} c_{\mathbf{i}}(t) \boldsymbol{\Psi}_{\mathbf{i}}(\boldsymbol{\xi}) \right) \rho(\boldsymbol{\xi}) d\xi = c_0, \tag{8}$$

The covariance matrix Σ can be obtained as follows:

$$\begin{aligned} \Sigma &= \mathbb{E}[(\mathbf{X}(t, \boldsymbol{\xi}) - \bar{\mathbf{X}}(t, \boldsymbol{\xi}))^2] & (9) \\ &\approx \int_{\Omega_{\boldsymbol{\xi}}} \left(\sum_{\mathbf{i},|\mathbf{i}|\neq 0} \mathbf{c}_{\mathbf{i}}(t) \boldsymbol{\Psi}_{\mathbf{i}}(\boldsymbol{\xi})) \right) \cdot \left(\sum_{\mathbf{i},|\mathbf{i}|\neq 0} \mathbf{c}_{\mathbf{i}}(t) \boldsymbol{\Psi}_{\mathbf{i}}(\boldsymbol{\xi})) \right) \rho(\boldsymbol{\xi}) d\xi & (10) \\ &= \sum_{\mathbf{i},|\mathbf{i}|\neq 0} \langle \boldsymbol{\Psi}_{\mathbf{i}}^2 \rangle \, \mathbf{c}_{\mathbf{i}} \mathbf{c}_{\mathbf{i}}^T(t). & (11) \end{aligned}$$

Similar expressions also exists for higher moments of the distribution.

To incorporate the random process $W(t, \omega)$ into the polynomial expansion, a Karhunen-Loève expansion (KLE) is used:[28]

$$\tilde{W}(t,\omega) \approx \bar{W}(t,\omega) + \sum_{n=1}^{M} \sqrt{\lambda_n}\theta_n(\omega) f_n(t), \tag{12}$$

where $\bar{W}(t,\omega)$ is the mean process, the coefficients $\theta_n(\omega)$ are a set of random variables, M is the truncation order, and λ_n and f_n are eigenvalues and eigenfunctions of the autocovariance kernel, which is given by:

$$K_W(s,t) = \mathbb{E}[(\mathbf{X}(s,\boldsymbol{\xi}) - \bar{\mathbf{X}}(s,\boldsymbol{\xi})(\mathbf{X}(t,\boldsymbol{\xi})) - \bar{\mathbf{X}}(t,\boldsymbol{\xi})^T]. \tag{13}$$

The KLE transforms the random process into a sum of random variables, which can be used by the PCE. In that case, the uncertainty vector $\boldsymbol{\xi}$ is appended with $\theta_n(\omega)$ and the point collocation samples are propagated using Eq. (1) where the random process is substituted by Eq. (12).

For a Gaussian random process, standard expressions for λ_n and f_n exist, and $\theta_n(\omega)$ are distributed as independent standard Gaussian random variables.[29] For the PCE, this means that order-1 Hermite polynomials can be used to expand these variables. However, when the process is non-Gaussian, the joint distribution of $\theta_n(\omega)$ is generally not Gaussian and hard to determine. Various works have shown that PCE can also be used to simulate non-Gaussian processes by expanding the coefficients using other types of polynomials that correspond to the desired statistical properties of the random process.[30,31] In this work Gaussian processes are considered as an initial proof-of-concept and because it allows for straightforward performance comparisons. However, no generality is lost as a change in the choice of polynomial basis can be used to approximate other random processes without changing the underlying methodology.

The main difficulty in the implementation of the PCE and KLE is that the approximation error of both grows as the propagation time increases. An example of this can be seen in Figure 1, where the error over time is shown for different KLE orders. The growth of this error can be controlled by increasing the order of the expansion or the amount of KLE coefficients, but this in turn increases the amount of samples required to build the approximation, leading to low numerical efficiency. Instead, the approach developed in[32] and[33] is adopted. This method, called dynamical polynomial chaos, divides the propagation time into a set of shorter time windows. Within these time windows, the PCE samples are propagated as normal until the end of the window. After this, the expansion is re-initialized, taking the final state distribution at the end of the previous window as the new initial state distribution. This is possible due to the Markovian property of the KLE considered here, which results in the KLE coefficients being independent on their value during the previous time window. As the accuracy of the KLE is dependent on the amount of coefficients used and the length of the time window, see Figure 1, a lower amount of samples can be used while retaining a similar level of accuracy. However, the final distribution at the end of each time window is not necessarily independent anymore, which is a requirement for constructing the orthogonal polynomials of Eq. (4). To resolve this, at the end of each window a new set of orthogonal polynomials is constructed using the Gram-Schmidt process as described in.[8]

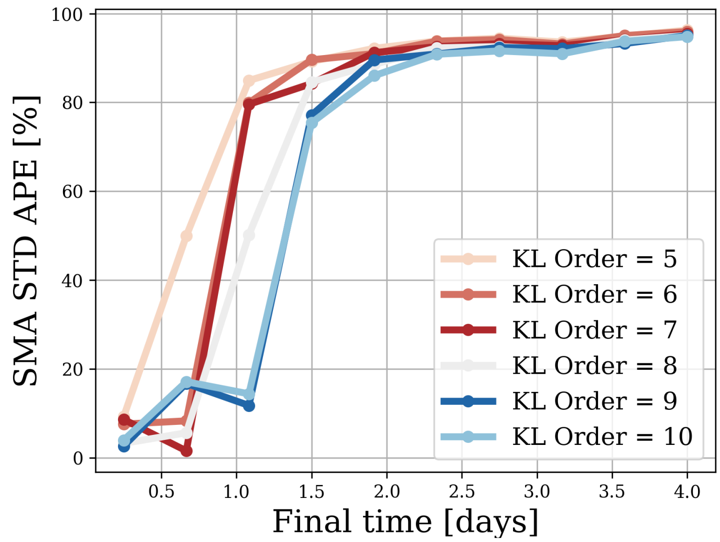

Figure 1: The accuracy of the estimated standard deviation using KLE for different final times.

Pseudo-diffusion Indicator

The pseudo-diffusion indicator is based on the fact that for a generic random-walk like process in the univariate-case, the mean-squared displacement of an ensemble of trajectories grows according to the following equation:[34]

$$\sigma^2 = \mathbb{E}[(x(t) - \bar{x}(t))^2] \approx K_\gamma t^\gamma, \tag{14}$$

where K_γ is the diffusion coefficient, γ the diffusion exponent, and $\bar{x}$ is a reference position. For simple Brownian motion, the exponent γ is equal to one leading to normal diffusion of the process. However, there are several conditions under which γ is not equal to 1, which is called anomalous diffusion. More specifically, $\gamma < 1$ is called subdiffusion and $\gamma > 1$ is called superdiffusion. Anomalous diffusion can come about due to properties of the dynamical system like chaos,[35] or non-Brownian effects in the random process.[34]

Combining the expression for the polynomial expansion variance in Eq. (11) (simplifying to the univariate case) with Eq. (14) gives the following expression:

$$\sum_{\mathbf{i},|\mathbf{i}|\neq 0} \kappa_{\mathbf{i}}\, c_{\mathbf{i}}^2(t) = K_\gamma t^\gamma, \tag{15}$$

Assuming large t, γ can be approximately found using the following expression:

$$\gamma \approx \tilde{\gamma} = \frac{\log\left(\sum_{\mathbf{i},|\mathbf{i}|\neq 0} \kappa_{\mathbf{i}}\ c_{\mathbf{i}}^2(t) + 1\right)}{\log t} \tag{16}$$

Where $\tilde{\gamma}_o$ is called the pseudo-diffusion exponent. This expression can be extended to the multivariate case again as follows:

$$\tilde{\gamma} = \frac{\log\left(\sqrt{\max_i \lambda_i(\mathbf{c}(t))} + 1\right)}{\log t}, \tag{17}$$

where λ_i is the ith eigenvalue of the covariance matrix Σ. This equation for $\tilde{\gamma}$ is fully defined by the coefficients of the polynomial approximation of the dynamics and its relation with the diffusive process of Eq. (14). It shows that the coefficients and its evolution over time can characterize the effect of the uncertainties on the dynamical system.

RESULTS

As an example case, the motion of a particle around an asteroid with a significant non-spherical gravitational perturbation is considered. This case shows both the capability of the methodology to deal with highly non-linear dynamics, and can be seen as a relevant system due to the fact that the evolution of clouds of particles around these systems are governed both by the complex gravitational field and inter-particle collisions and gravitational attraction.

Resonances play a crucial role in this dynamical environment due to the influence of the asteroid's non-spherical gravitational potential. Understanding these resonant structures is essential for exploring the dynamical pathways that determine whether particles become temporarily trapped in resonant zones or are eventually lost from the system. For this work, we focus on the 3:1 resonance around the Didymos asteroid. Didymos is an interesting case as one of the hypotheses is that ejecta coming from the surface formed a ring of material which moved around the system until it formed a moonlet, which now is observed to be the secondary Dimorphos.[36] Therefore, a accurate dynamical model that incorporates the stochastic interactions within the ring is of great importance. The 3:1 resonance specifically is investigated because, in the planar case ($i = 0°$), it consistently appears in the phase space across a range of eccentricities and is among the resonances associated with the largest resonance islands. Furthermore, for the few observed asteroid rings, e.g. Chariklo and Haumea, the 3:1 resonance plays a key role in the ring dynamics.[37]

Several initial conditions in the (M, a) phase space, where M is the mean anomaly and a is the semi-major axis (SMA), are propagated over a period of 10 days. The gravitational potential of the body is modeled using spherical harmonics up to degree and order 6, in order to capture the effects of its irregular shape. The choice of the phase space is motivated by its close analogy to resonant phase space maps commonly used in the study of resonant motion around irregularly shaped bodies. In this context, the mean anomaly can be associated with the resonant angle $\sigma =$

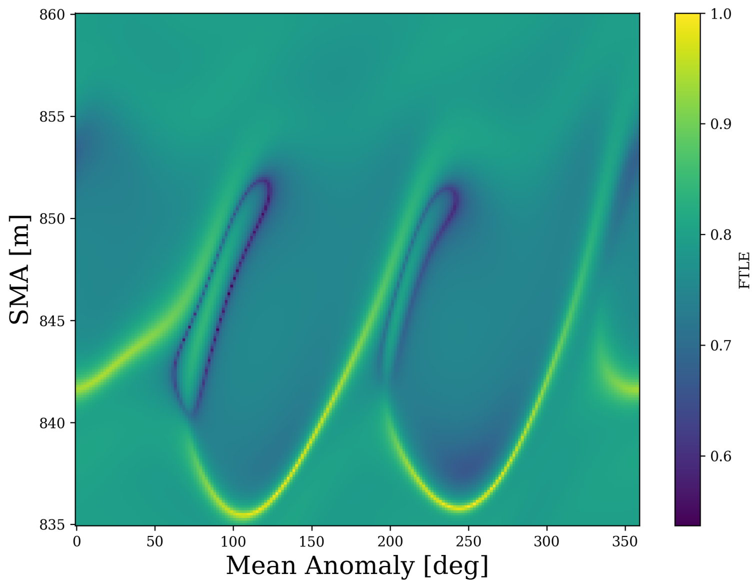

Figure 2: The FTLE map of the 1:3 resonance around Didymos.

$p_2(M + \Omega + \omega) - p_1\theta$, with $p_2 : p_1$ giving commensurability condition for a resonance to occur around a rotating primary.

Using Kaula's formulation for the Hamiltonian, one typically obtains pendulum-like structures in the (M, a) space that clearly distinguish regions of circulation from regions of libration. In this study, a similar approach is adopted: instead of relying solely on the analytical Hamiltonian, we compute Finite-Time Lyapunov Exponents (FTLEs) based on direct numerical integration of the equations of motion to identify chaotic and regular regions in the phase space. The equations of motion are given by:

$$\ddot{\mathbf{r}} = -2\dot{\theta} \times \dot{\mathbf{r}} - \dot{\theta} \times (\dot{\theta} \times \mathbf{r}) - \nabla U \tag{18}$$

with

$$U = -\frac{GM}{r}\sum_{n=0}^{\infty}\sum_{m=0}^{m}\frac{R_b^n}{r^n}P_{nm}sin(\phi)(\bar{C}_{nm}cos(m\lambda) + \bar{S}_{nm}sin(m\lambda)) \tag{19}$$

The resulting FTLE map for Didymos is shown in Figure 2. It can be observed that there are a clear set of three regions with low FTLE values which are contained within ridges of high FTLE values, i.e. the separatrixes. This clearly shows the effect of resonances in the dynamics, creating possible regions where trajectories can end up and remain stable over longer periods of time.[38] Hence, in the following it will be analyzed how a stochastic process influences this type of dynamics.

However, first the accuracy of the proposed methodology needs to be determined. For this, a set of 100 trajectories starting from $(M, a) = (0.0°, 850 \text{ m})$ are taken and propagated for 10 days. A linear diffusion function is used, where only planar accelerations are considered (due to the planar nature of rings):

$$\mathbf{G}(\mathbf{X}(t, \omega), t) = \begin{pmatrix} \sigma_x, 0, 0 \\ \\ 0, \sigma_y, 0 \\ \\ 0, 0, 0 \end{pmatrix}. \tag{20}$$

The σ values can be tuned to represent collisions and other interactions for specific ring densities and velocity dispersions. For the testing done here a value of $\sigma_x = \sigma_y = 1e - 4$ was used. The trajectories which will be considered as true values are propagated in two different ways. First, the KLE expansion is used to represent the stochastic process and each sample trajectory represents a different set of samples of θ_n. The second method is a stochastic numerical integrator that is adapted from the classical Runge-Kutta method,[39] i.e. a stochastic Runge-Kutta (SRK) method. The second method is used besides the KLE method to have a method that tests both the accuracy of the DPCE and KLE combined.

Figure 3 shows the results of the accuracy analysis. Figures 3a and 3b show both the DPCE and MC evolution of the SMA and eccentricity over time where the KLE was used. It can be seen that both the mean and 3σ bounds of the DPCE method follow the MC well, with mainly at the start the variance of the SMA being underestimated. Figures 3c and 3d on the other hand show the results compared to the MC using SRK. The mean of both the SMA and eccentricty for this case remain close to each other, showing that the general behaviour is captured well. The variance in this case is less accurate then before, as the truncation error of the KLE is added to the DPCE error. However, the qualtitative behaviour is still very similar and the diffusion of trajectories over time is captured well. Thus, it can be concluded that the DPCE method works well and can be taken to be accurate for the measurement of the influence of the stochastic process.

Figure 4 shows the pseudo-diffusion indicator map calculated for three different levels of stochasticity, represented by $\sigma = \sigma_x = \sigma_y$. Figure 4a shows the map for $\sigma = 1e - 4$. Here it can be observed that most of the structures that can be found for the deterministic system shown in Figure 2, still remain. The level of stochasticity is low enough that the deterministic dynamics dominate. Once we increase the stochasticity, as shown in Figure 4b and Figure 4c, the dynamics start to change significantly. The seperatrixes mainly remain as they have a strong diffusive effect, but the stable regions in between are shown to become more unstable. Thus, in case of rings or other situations where there are more high energy impacts between orbiting particles, the possibility of capture in these resonances might become less likely.

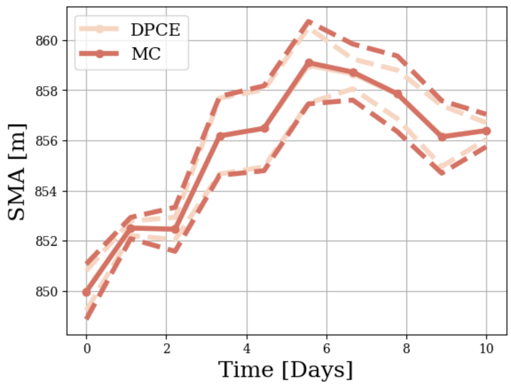

(a) SMA with KLE.

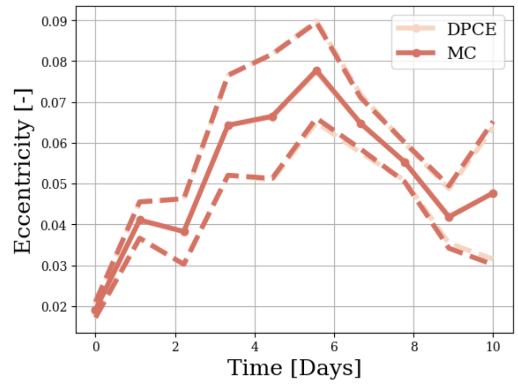

(b) Eccentricity with KLE.

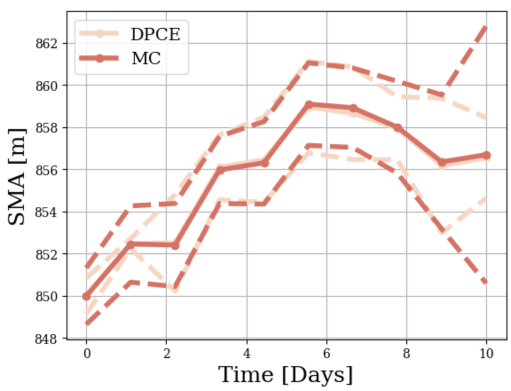

(c) SMA without KLE.

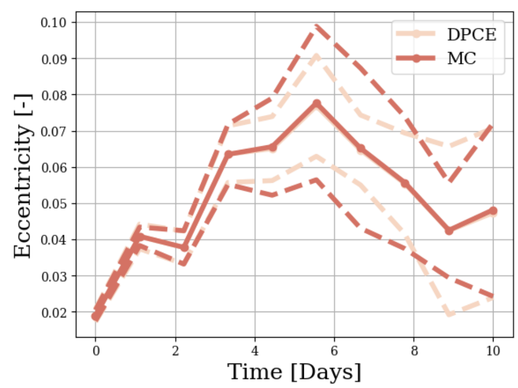

(d) Eccentricity without KLE.

Figure 3: Comparison between the proposed DPCE methodology and a MC analysis. The solid lines are the mean and the dashed lines the 3σ bounds. The upper figures show the comparison when a KLE was used to propagate the MC samples and the lower figures show for when a Stochastic Runge-Kutta method was used.

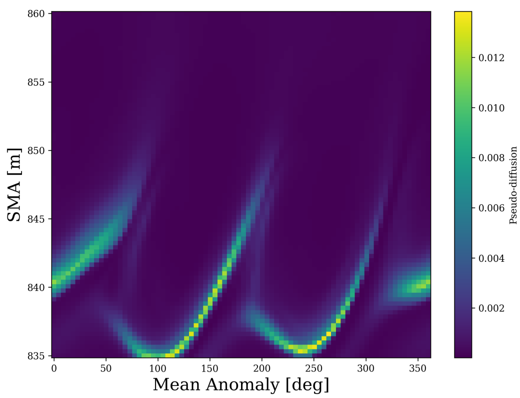

(a) $\sigma = 1e-4$.

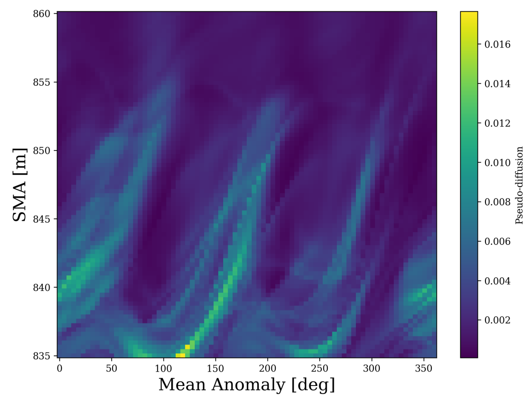

(b) $\sigma = 5e-4$.

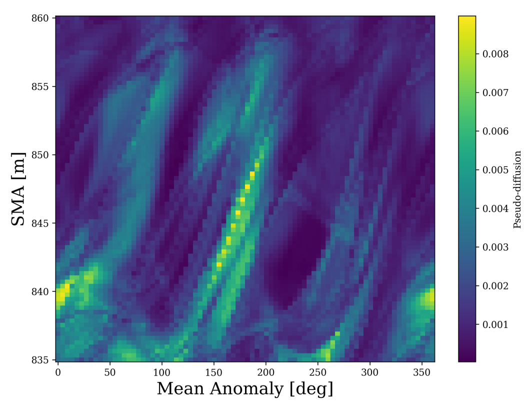

(c) $\sigma = 1e-3$.

Figure 4: Pseudo diffusion indicator maps for different levels of stochasticity.

CONCLUSION

This work aims to do two things: present the importance of stochastic processes in astrodynamics and celestial mechanics, and provide a framework for analysing these systems. It was identified that most of these stochastic processes involve either a large amount of low-velocity impacts or hyperbolic encounters with larger bodies. The characterization methodology is based on the polynomial chaos expansion (PCE), which expands the solution of the stochastic dynamics and provide an analytical expression for the state distribution at future times. Specifically, a dynamical indicator, representing the degree of diffusion, can be calculated for different initial conditions to determine properties like stability and chaos.

It is shown that using the pseudo diffusion indicator maps can be made of the resonance regions in non-spherical potentials. The specific level of stochasticity was found for when the resonance regions become unstable and capture into these regions becomes less likely.

Concluding, the presented methodology is shown to be very effective for characterising stochastic dynamics, even in complex environments like small Solar system bodies. Thus, this tool can be used in future work to design safer space missions and investigate further many dynamical processes in the Solar system.

ACKNOWLEDGMENT

This work was partly carried out within the Space It Up! project funded by the Italian Space Agency (ASI) and the Italian Ministry of University and Research (MUR) under contract No. 2024-5-E.0, CUP No. I53D24000060005. Partly funded by the European Union (ERC, TRACES, 101077758). Views and opinions expressed are however those of the author(s) only and do not necessarily reflect those of the European Union or the European Research Council. Neither the European Union nor the granting authority can be held responsible for them.

REFERENCES

[1] L. B. Sagnières and I. Sharf, “Stochastic modeling of hypervelocity impacts in attitude propagation of space debris,” *Advances in Space Research*, Vol. 59, 2 2017, pp. 1128–1143, 10.1016/J.ASR.2016.11.030.

[2] B. Sicardy, M. El Moutamid, S. Renner, R. Sfair, and D. Souami, “Origins of rings in the Solar System,” *Philosophical Transactions A*, Vol. 383, 2 2025, 10.1098/RSTA.2024.0193.

[3] F. C. Adams and A. M. Bloch, “General Analysis of Type I Planetary Migration with Stochastic Perturbations,” *The Astrophysical Journal*, Vol. 701, 7 2009, p. 1381, 10.1088/0004-637X/701/2/1381.

[4] E. Belbruno and J. R. Gott III, “Where Did the Moon Come From?,” *The Astronomical Journal*, Vol. 129, 3 2005, pp. 1724–1745, 10.1086/427539.

[5] S. N. Sharma and H. Parthasarathy, “Dynamics of a stochastically perturbed two-body problem,” *Proceedings of the Royal Society A: Mathematical, Physical and Engineering Sciences*, Vol. 463, 4 2007, pp. 979–1003, 10.1098/RSPA.2006.1801.

[6] F. Pierret, “Stochastic Gauss equations,” *Celestial Mechanics and Dynamical Astronomy*, Vol. 124, 2 2016, pp. 109–126, 10.1007/S10569-015-9652-1/FIGURES/5.

[7] E. Belbruno, “Random walk in celestial mechanics,” *Regular and Chaotic Dynamics*, Vol. 14, 2 2009, pp. 7–17, 10.1134/S1560354709010031/METRICS.

[8] M. Manzi and M. Vasile, "Analysis of Stochastic Nearly-integrable Dynamical Systems using Polynomial Chaos Expansions," *2020 AAS/AIAA Astrodynamics Specialist Conference*, South Lake Tahoe, 2020.

[9] B. Øksendal, *Stochastic Differential Equations*. Universitext, Berlin, Heidelberg: Springer Berlin Heidelberg, 6 ed., 2003, 10.1007/978-3-642-14394-6.

[10] C. Giordano, "A Deterministic-Stochastic Hybrid Integrator for Random Ordinary Differential Equations with Aerospace Applications," *Aerospace 2025, Vol. 12, Page 397*, Vol. 12, 4 2025, p. 397, 10.3390/AEROSPACE12050397.

[11] H. Rein and J. C. B. Papaloizou, "Stochastic orbital migration of small bodies in Saturn's rings," *Astronomy & Astrophysics*, Vol. 524, 12 2010, p. A22, 10.1051/0004-6361/201015177.

[12] R. A. Murray-Clay and E. I. Chiang, "Brownian Motion in Planetary Migration," *The Astrophysical Journal*, Vol. 651, 11 2006, pp. 1194–1208, 10.1086/507514/FULLTEXT/.

[13] B. F. Collins and R. Sari, "Lévy Flights of Binary Orbits due to Impulsive Encounters," *The Astronomical Journal*, Vol. 136, 11 2008, p. 2552, 10.1088/0004-6256/136/6/2552.

[14] A. Hermosillo Ruiz, H. C. Lau, and R. Murray-Clay, "Randomness and retention: using weak mean motion resonances to constrain Neptune's late-stage migration," *Monthly Notices of the Royal Astronomical Society*, Vol. 531, 5 2024, pp. 1613–1629, 10.1093/MNRAS/STAE1246.

[15] E. B. Palmer IV, *Stochastic Satellite Air Drag with the Ballistic Coefficient as a Random Variable*. PhD thesis, Air Force Institute of Technology, 9 2021.

[16] C. R. Gates, "A Simplified Model of Midcourse Maneuver Execution Errors," tech. rep., Jet Propulsion Laboratory, Pasadena, 1963.

[17] S. G. Hesar, D. J. Scheeres, and J. W. McMahon, "Sensitivity analysis of the OSIRIS-REx terminator orbits to maneuver errors," *Journal of Guidance, Control, and Dynamics*, Vol. 40, 10 2017, pp. 81–95, 10.2514/1.G002058;REQUESTEDJOURNAL:JOURNAL:JGCD;ISSUE:ISSUE:10.2514/JGCD.2017.40.ISSUE-1.

[18] T. A. Springer, G. Beutler, and M. Rothacher, "A new solar radiation pressure model for GPS," *Advances in Space Research*, Vol. 23, 1 1999, pp. 673–676, 10.1016/S0273-1177(99)00158-1.

[19] M. Pan, H. Rein, E. Chiang, and S. N. Evans, "Stochastic flights of propellers," *Monthly Notices of the Royal Astronomical Society*, Vol. 427, 12 2012, pp. 2788–2796, 10.1111/J.1365-2966.2012.22023.X/2/M_427-4-2788-IEQ072.JPEG.

[20] H. Salo and B. Sicardy, "Collisional confinement of 1:3 resonance ringlets around non-spherical bodies," *Europlanet Science Congress 2024*, Berlin, 9 2024, 10.5194/EPSC2024-534.

[21] J. S. Oishi, M. Mac Low, and K. Menou, "Turbulent Torques on Protoplanets in a Dead Zone," *The Astrophysical Journal*, Vol. 670, 11 2007, pp. 805–819, 10.1086/521781/FULLTEXT/.

[22] L. Y. Zhou, Y. S. Sun, J. L. Zhou, J. Q. Zheng, and M. Valtonen, "Stochastic effects in the planet migration and orbital distribution of the Kuiper Belt," *Monthly Notices of the Royal Astronomical Society*, Vol. 336, 10 2002, pp. 520–526, 10.1046/J.1365-8711.2002.05768.X.

[23] A. Hermosillo Ruiz, L. Harriet, and R. Murray-Clay, "The Impact of Stochastic Migration on Weak Resonances in The Kuiper Belt," *AAS Division on Dynamical Astronomy meeting*, Vol. 53, 2021.

[24] A. Cano, M. Sanjurjo-Rivo, J. Míguez, A. Pastor, and D. Escobar, "Atmospheric drag uncertainty quantification for orbit determination and propagation via Stochastic Consider Parameters," *Advances in Space Research*, Vol. 75, 6 2025, pp. 8667–8686, 10.1016/J.ASR.2025.04.018.

[25] C. Giordano, "Characterization of Gauss–Markov stochastic sequences for mission analysis," *Astrodynamics*, Vol. 8, 3 2024, pp. 135–148, 10.1007/S42064-023-0183-3/METRICS.

[26] N. Wiener, "The Homogeneous Chaos," *American Journal of Mathematics*, Vol. 60, 10 1938, p. 897, 10.2307/2371268.

[27] D. Xiu and G. Em Karniadakis, "The Wiener-Askey Polynomial Chaos for Stochastic Differential Equations," *SIAM Journal on Scientific Computing*, Vol. 24, 7 2006, pp. 619–644, 10.1137/S1064827501387826.

[28] W. Betz, I. Papaioannou, and D. Straub, "Numerical methods for the discretization of random fields by means of the Karhunen–Loève expansion," *Computer Methods in Applied Mechanics and Engineering*, Vol. 271, 4 2014, pp. 109–129, 10.1016/J.CMA.2013.12.010.

[29] P. Deheuvels, "Karhunen-Loève Expansions of Mean-Centered Wiener Processes on JSTOR," 2006.

[30] J. N. Mueller, K. Sargsyan, C. J. Daniels, H. N. Najm, J. N. Mueller, K. Sargsyan, C. J. Daniels, and H. N. Najm, "Polynomial Chaos Surrogate Construction for Random Fields with Parametric Uncertainty," *SIAM/ASA Journal on Uncertainty Quantification*, Vol. 13, 11 2023, p. 2023, 10.1137/23M1613505.

[31] H. Dai, Z. Zheng, and H. Ma, "An explicit method for simulating non-Gaussian and non-stationary stochastic processes by Karhunen-Loève and polynomial chaos expansion," *Mechanical Systems and Signal Processing*, Vol. 115, 1 2019, pp. 1–13, 10.1016/J.YMSSP.2018.05.026.

[32] H. C. Ozen and G. Bal, "Dynamical polynomial chaos expansions and long time evolution of differential equations with random forcing," *SIAM-ASA Journal on Uncertainty Quantification*, Vol. 4, No. 1, 2016, pp. 609–635, 10.1137/15M1019167.

[33] C. Greco, M. Di Carlo, M. Vasile, and R. Epenoy, "Direct multiple shooting transcription with polynomial algebra for optimal control problems under uncertainty," *Acta Astronautica*, Vol. 170, 5 2020, pp. 224–234, 10.1016/j.actaastro.2019.12.010.

[34] S. B. Alves, G. F. De Oliveira, L. C. De Oliveira, T. Passerat De Silans, M. Chevrollier, M. Oriá, and H. L. S. Cavalcante, "Characterization of diffusion processes: Normal and anomalous regimes," *Physica A: Statistical Mechanics and its Applications*, Vol. 447, 4 2016, pp. 392–401, 10.1016/J.PHYSA.2015.12.049.

[35] Y. Sato and R. Klages, "Anomalous diffusion in random dynamical systems," *Physical Review Letters*, Vol. 122, 4 2019, p. 174101, 10.1103/PHYSREVLETT.122.174101/ADRDS_SUPP_RESUB2.PDF.

[36] J. Wimarsson, Z. Xiang, F. Ferrari, M. Jutzi, G. Madeira, S. D. Raducan, and P. Sánchez, "Rapid formation of binary asteroid systems post rotational failure: A recipe for making atypically shaped satellites," *Icarus*, Vol. 421, 10 2024, p. 116223, 10.1016/J.ICARUS.2024.116223.

[37] B. Sicardy, R. Leiva, S. Renner, F. Roques, M. El Moutamid, P. Santos-Sanz, and J. Desmars, "Ring dynamics around non-axisymmetric bodies with application to Chariklo and Haumea," *Nature Astronomy 2018 3:2*, Vol. 3, 11 2018, pp. 146–153, 10.1038/s41550-018-0616-8.

[38] W. Boumchita and J. Feng, "The capture probability of Dawn into ground-track resonances with Vesta," *Celestial Mechanics and Dynamical Astronomy*, Vol. 136, 2 2024, pp. 1–33, 10.1007/S10569-023-10175-Y/FIGURES/28.

[39] A. Rößler, "Runge-Kutta methods for the strong approximation of solutions of stochastic differential equations," *SIAM Journal on Numerical Analysis*, Vol. 48, 6 2010, pp. 922–952, 10.1137/09076636X;REQUESTEDJOURNAL:JOURNAL:SJNAAM;PAGEGROUP:STRING:PUBLICATION.